Mark A. Nixon*
Bruce C. McCallum
W. Richard Fright
and
N. Brent Price
Applied Research Associates NZ Ltd.
P.O. Box 3894
Christchurch, New Zealand

The Effects of Metals and Interfering Fields on Electromagnetic Trackers

Abstract

The operation of six degree-of-freedom electromagnetic trackers is based on the spatial properties of the electromagnetic fields generated by three small coils. Anything in the environment that causes these fields to be distorted will result in measurement noise and/or errors. An experimental investigation was undertaken to measure the effect of external fields present in a typical working environment (namely mains and computer monitor fields) and the presence of metals (25-mm cubes of various types of metals, a large steel bar, and a large steel sheet). A theoretical model is proposed to explain the observations. Two devices were used in this investigation: a Polhemus Fastrak and an Ascension Flock of Birds.

1 Introduction

Electromagnetic trackers (Raab et al., 1979) are electronic devices that determine the position and orientation (six degrees of freedom) of a receiver relative to a transmitter. They have been popular in a diversity of applications, from animation and virtual reality (Ellis, 1991; Meyer, Applewhite, and Biocca, 1992; Stone, 1996) to the military (Ferrin, 1991) and medical (Martin et al., 1993; Detmer et al., 1994) sectors.

Research into the performance of electromagnetic trackers has tended to concentrate on accuracy and latency issues (Bryson and Fisher, 1990; Liang, Shaw, and Green, 1991; Bryson, 1992; Adelstein, Johnston, and Ellis, 1992; Emura and Tachi, 1994; Wloka, 1995; Adelstein, Johnston, and Ellis, 1996). However many practical questions remain unanswered, especially in regard to their performance in the presence of metals or interfering fields (Barfield and Furness, 1995). Although some research has been performed in this area (Burdea, Dunn, Immendorf, and Mallik, 1991; Kato et al., 1991; Williams, 1993) the results have been either only qualitative or too detailed and lacking a model from which to draw any conclusions.

The aim of this paper is to present succinct, quantitative information and principles that the reader can apply when using these devices. To this end, we have undertaken an experimental investigation of the effects of metals and interfering fields, as may be present in a typical working environment. Simple theoretical models have been developed to explain the results. Note that this paper does not consider accuracy or latency; nor does it aim to show the

Presence, *Vol. 7, No. 2, April 1998*, 204–218

*Please direct written correspondence to: Mark Nixon at Applied Research Associates and electronic communication to him at m.nixon@aranz.co.nz

advantage of one type of tracker over another, as this result will depend on the particular application.

Two electromagnetic trackers have been used in this investigation; a Polhemus Fastrak[1] and an Ascension Flock of Birds.[2] In both systems the transmitter consists of three orthogonal coils that are energized sequentially to produce electromagnetic fields every measurement cycle. Each field produces a signal in the three orthogonal sensors contained in the receiver. Thus, each measurement cycle consists of at least nine signal measurements from which the six position and orientation components are calculated.

They differ, however, in the manner in which the fields are generated and detected. The Fastrak transmitter is energized by bursts of sinusoidal current (carrier frequency of 8, 10, 12, or 14 kHz), and the receiver contains passive coils in which currents are induced. Hence, the Fastrak is referred to as an AC system. The Bird's transmitter, however, is energized by rectangular pulses of direct current, and the receiver consists of orthogonal fluxgate sensors that measure the field. The Bird is thus a quasi-DC system, and as a consequence must make three additional passive measurements per cycle in order to compensate for the constant magnetic field of Earth. Note that the interval over which each coil is energized is fixed in the case of the Fastrak, but varies in proportion to the duration of the measurement cycle for the Bird.

In Section 2 a simple mathematical model of an electromagnetic tracker is described, and in Section 3 the parameters that were measured in the experiments are explained. Sections 4 and 5 contain details of the experiments performed to investigate the effects of interfering fields and metals, respectively. Conclusions are drawn in Section 6.

1. Polhemus Incorporated, Colchester, Vermont, USA
2. Ascension Technology Corporation, Burlington, Vermont, USA

2 Predicted Behavior

The potential field v at a distance r from a coil transmitter are related by (Ramo, Whinnery, and Duzer, 1965, p. 122):

$$v \propto r^{-3} \tag{1}$$

The operation of both trackers is effectively based on inverting (1) to determine the transmitter–receiver separation, i.e.,

$$r \propto v^{-1/3} \tag{2}$$

An error Δr in the calculation of r due to an error Δv in the measurement of v, (i.e., the sensitivity), is related to the derivative of (2), i.e.,

$$\Delta r \propto \frac{dr}{dv}\Delta v \tag{3}$$

$$\rightarrow \Delta r \propto r^4 \Delta v \tag{4}$$

So, in the case of an interfering electromagnetic field at a fixed distance from the receiver (i.e., constant Δv) we can expect the error in the calculated position to be proportional to the fourth power of the transmitter–receiver separation d_{tr}, i.e.,

$$\Delta r \propto {d_{tr}}^4 \tag{5}$$

In the case where metal is present in the vicinity of the tracker, the transmitter's field will induce eddy currents in the metal whose amplitude, according to (1), is proportional to the inverse cube of the transmitter–metal separation, d_{tm}. Similarly, the measured potential field due to the eddy current is proportional to the inverse cube of the metal–receiver separation, d_{mr}. Thus, the measurement error Δv is related by

$$\Delta v \propto \frac{1}{{d_{tm}}^3 {d_{mr}}^3} \tag{6}$$

After (4) and (6) are combined, the error in the calculated position due to a metal object is predicted to be

$$\Delta r \propto \frac{{d_{tr}}^4}{{d_{tm}}^3 {d_{mr}}^3} \tag{7}$$

Ferromagnetic materials are a particular problem be-

cause, in addition to an eddy current field, a magnetization field is produced due to the high permeability of those materials. The distortion due to the magnetization field is also adequately modeled by (7).

3 Performance Parameters

The trackers return six output parameters to describe the location and orientation of the receiver with respect to the transmitter: three Cartesian coordinates, x, y, and z to describe the position, and three Euler angles, θ_z (azimuth), θ_y (elevation), and θ_x (roll) to describe the orientation. A 3×3 rotation matrix $\mathbf{M}$ can be used to describe the orientation instead of the Euler angles.

A convenient way of expressing these parameters is in terms of the receiver position vector $\mathbf{r}$, where

$$\mathbf{r} = [x, y, z]^{\mathrm{T}} \tag{8}$$

and a pointer position $\mathbf{p}$, which is the tip of an imaginary pointer attached to the receiver. The pointer position $\mathbf{p}$ is determined by the length l of the pointer and the orientation of the receiver (in terms of Euler angles or matrix $\mathbf{M}$), i.e.,

$$\mathbf{p} = l\mathbf{M}\mathbf{v} \tag{9}$$

where the unit vector $\mathbf{v}$ has an arbitrary direction, e.g., $\mathbf{v} = \frac{1}{\sqrt{3}}[1, 1, 1]^{\mathrm{T}}$. A pointer length of $l = 500$ mm was used throughout, although the pointing error scales linearly for other pointer lengths. Such an approach has been used elsewhere (Detmer et al., 1994), although this formulation is insensitive to rotation about the pointer.

In the following sections, the effects of metals and interfering fields are reported in terms of the error and/or noise present on the two parameters $\mathbf{r}$ and $\mathbf{p}$. In each of the experiments the measurements were repeated N times, typically 1000. The scalar position error, e_r, and pointing error, e_p, are defined by

$$e_r = |\bar{\mathbf{r}} - \bar{\mathbf{r}}_0| \tag{10}$$

$$e_p = |\bar{\mathbf{p}} - \bar{\mathbf{p}}_0| \tag{11}$$

where $\bar{\mathbf{r}}$ and $\bar{\mathbf{p}}$ denote the mean values of $\mathbf{r}$ and $\mathbf{p}$ for the N measurements, and where $\bar{\mathbf{r}}_0$ and $\bar{\mathbf{p}}_0$ denote $\bar{\mathbf{r}}$ and $\bar{\mathbf{p}}$ measured in the absence of the distorting effect under investigation.

The RMS (root mean square) noise σ_r and σ_p in the position and pointing measurements, respectively, are defined by

$$\sigma_r = \sqrt{\frac{1}{N}\sum_{n=1}^{N} |\mathbf{r}_n - \bar{\mathbf{r}}|^2} \tag{12}$$

$$\sigma_p = \sqrt{\frac{1}{N}\sum_{n=1}^{N} |\mathbf{p}_n - \bar{\mathbf{p}}|^2} \tag{13}$$

4 Effects of Interfering Fields

Because the magnetic trackers are based on electromagnetic fields, they are susceptible to interference from neighboring external sources of fields. Experiments were performed to investigate the effects of interfering fields present in a typical working environment. The experimental environment consisted of a ground floor room in an office building, with fluorescent lighting, a computer and minor electrical devices powered up. The tracker's transmitter and receiver were supported on a metal-free bench one meter high and at least two meters from any wall or other device. The chief sources of interference were therefore expected to be mains reticulation and the nearby computer monitor.

Four effects were investigated as described in the following subsections. First, the relationship between mains-induced noise on the tracker measurement and the frequency at which the tracker was sampled was examined, for a wide range of sampling frequencies including mains-synchronous sampling. The effect of two-tap filtering at each sampling frequency was also considered. Second, the relative benefits of synchronizing to the vertical refresh frequency of the nearby computer monitor compared with asynchronous or mains-synchronous sampling, and the dependence on monitor–receiver separation, was investigated. Thirdly, the error produced when the tracker's own transmitter and receiver leads were in close proximity was examined. Finally, the relationship between noise magnitude and transmitter–

receiver separation, (i.e., the noise sensitivity of these devices), was investigated and compared with that predicted by the model developed in Section 2.

4.1 Mains Interference and Sampling Frequency

The most ubiquitous source of electromagnetic interference in an office environment is likely to be the field generated by mains-powered appliances and reticulation. To investigate this effect, the transmitter and receiver were rigidly fixed 600 mm apart, and the RMS position and pointing noise on the unfiltered tracker measurements were recorded for various tracker sampling frequencies (denoted by f_s). The term ''sampling frequency'' refers here to the measurement cycle, i.e., the rate at which new tracker output records are produced. Results are shown in Figure 1 (solid lines).

The Fastrak and Bird have quite different susceptibilities to external field interference. This is because the Fastrak is an AC system with a one kilohertz bandwidth centered at 8, 10, 12, or 14 kHz, whereas the Bird is a quasi-DC system with a bandwidth whose lower end extends down to near DC. In our office environment, where the external fields are predominantly due to mains reticulation, the Bird was more severely affected than the Fastrak, the latter exhibiting very low noise in the presence of ambient mains fields regardless of the sampling frequency. This may not be the case in other operating environments.

Recall from Section 1 that each measurement cycle involves three separate bursts of excitation and simultaneous sensor measurement (plus an extra passive sensor measurement in the case of the Bird). A consequence of this is that it is not possible to filter the sensor signals before sampling. Thus, there is the potential for aliasing of noise or actual tracker movement with frequencies in excess of half the sampling frequency. To avoid aliasing mains interference (of frequency f_m), one must choose $f_s \geq 2f_m$.

The choice of sampling frequency will depend on the requirements of each particular application. However, if external fields of significant levels are present, this may force a choice of higher sampling frequency and subsequent filtering.

The tracker measurements may be filtered either externally or preferably internally with inbuilt tracker func-

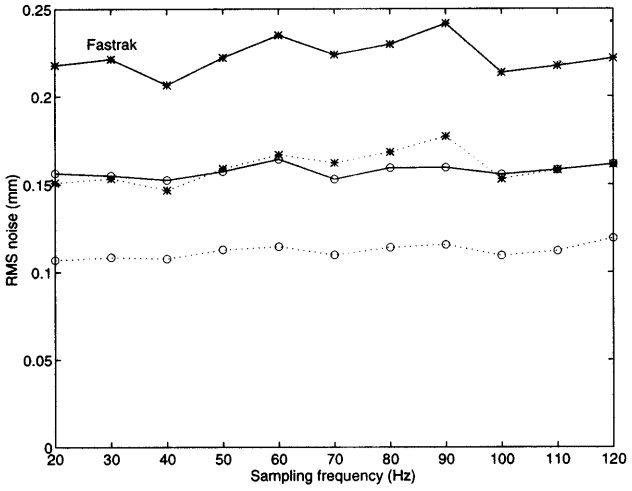

(a)

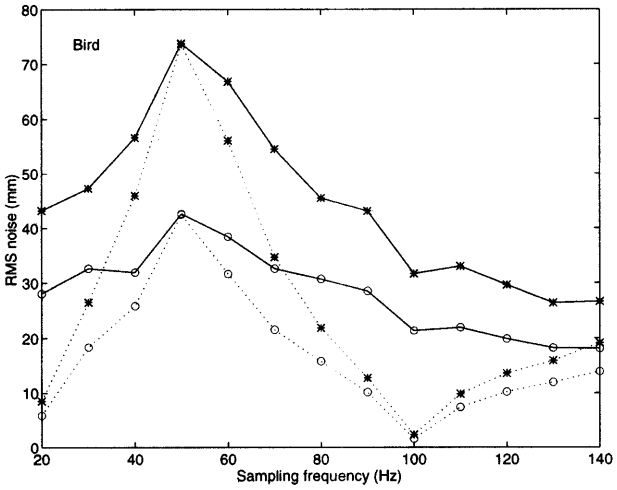

(b)

Figure 1. *The effect of sampling frequency on mains interference on position RMS noise "*" and pointing RMS noise "o" for (a) Fastrak and (b) Bird. The solid lines represent unfiltered data and the dotted lines represent filtered (two-tap) data. The maximum at 50 Hz and minimum at 100 Hz would occur at 60 Hz and 120 Hz, respectively, in North America. Note that the vertical scales of the two graphs are different.*

tions. If one chooses $f_s = 2f_m$, then a simple two-tap filter (i.e., averaging adjacent samples) significantly reduces the mains signal, especially in the case of the Bird, as demonstrated in Figure 1(b) (dashed lines). Note that the maximum at 50 Hz and minimum at 100 Hz would occur at 60 Hz and 120 Hz, respectively, in North America.

However, the mains frequency is not constant, varying slightly about f_m. If a constant frequency (e.g., crystal) source is used for f_s, the mains interference may not be entirely eliminated because f_m will vary about the zero of the filter transfer function ($f_s/2$). Furthermore, low-frequency beating can result, due to the mains second harmonic being aliased down towards DC; this beating may produce objectionable results in some applications. To effectively eliminate the mains interference it is necessary to synchronize the tracker sampling to the mains supply, as demonstrated in Section 4.2.

Hence, in the remaining sections, unless otherwise stated, both trackers have been sampled synchronously at twice mains frequency with two-tap filtering.

In most applications, it would be necessary to employ some form of filtering with the Bird to attenuate the mains interference. Whether mains synchronizing is necessary depends both on the requirements of the application and on the expected level of mains frequency variations.

Higher-order filters (either internal or external) can also be used, but whether this use is appropriate will depend on the requirements of the application (such as the expected frequency spectrum of the receiver movement). Both trackers provide inbuilt, nonlinear (DC) filters to reduce noise while attempting to maintain measurement bandwidth. However these issues are not discussed here, but can be found elsewhere, for example, in Adelstein et al. (1996).

These results are very dependent on transmitter–receiver separation due to (4). A separation of 600 mm was chosen for the experiment because it is a typical working distance for many applications. However, smaller separations will greatly decrease the noise in the presence of an interfering field (see Section 4.4).

4.2 Monitor or Mains Synchronization

The second most ubiquitous source of electromagnetic interference in the tracker's environment is likely to be the field generated by the cathode ray tube of a computer monitor. To investigate this effect, the transmitter and receiver were rigidly fixed 600 mm apart and a monitor was placed at various distances from the receiver on a line perpendicular to the transmitter–receiver axis, and positioned with the monitor screen towards the receiver. The monitor was a standard, low-emission 17″ CRT computer monitor running at a vertical refresh rate of approximately 70 Hz. The experimental setup is shown in Figure 2.

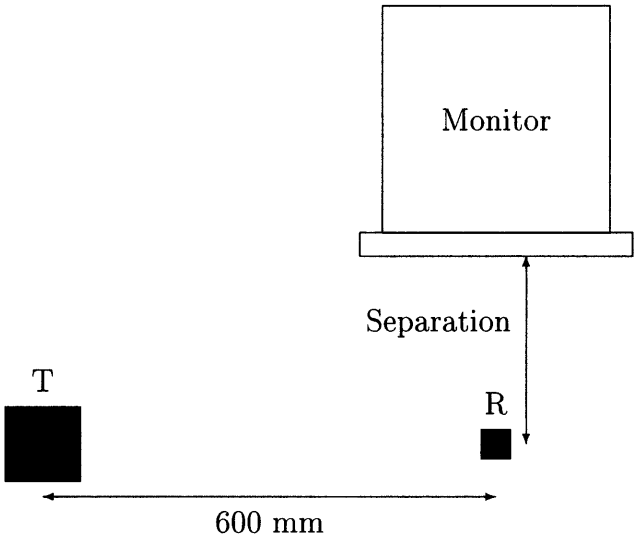

Figure 2. *Schematic diagram of the monitor interference experiment. The transmitter (T) and receiver (R) were securely fixed and separated by 600 mm. The receiver–monitor separation was varied.*

The experiment was repeated twice for each tracker; first with the sampling frequency synchronized to the monitor vertical refresh frequency using the pickup coil provided by the tracker manufacturer, and second with the sampling rate synchronized to the mains using a zero-crossing detector circuit. In all cases the RMS noise and error in the position measurement was determined. For the case of the Fastrak synchronized to the monitor, the sampling frequency was synchronized to the monitor frequency. (The Fastrak is unable to sample at twice the monitor frequency.) For the other three cases, the tracker sampling frequency was synchronized to twice the monitor or mains frequency, and two-tap filtering was employed. The results are shown in Figure 3.

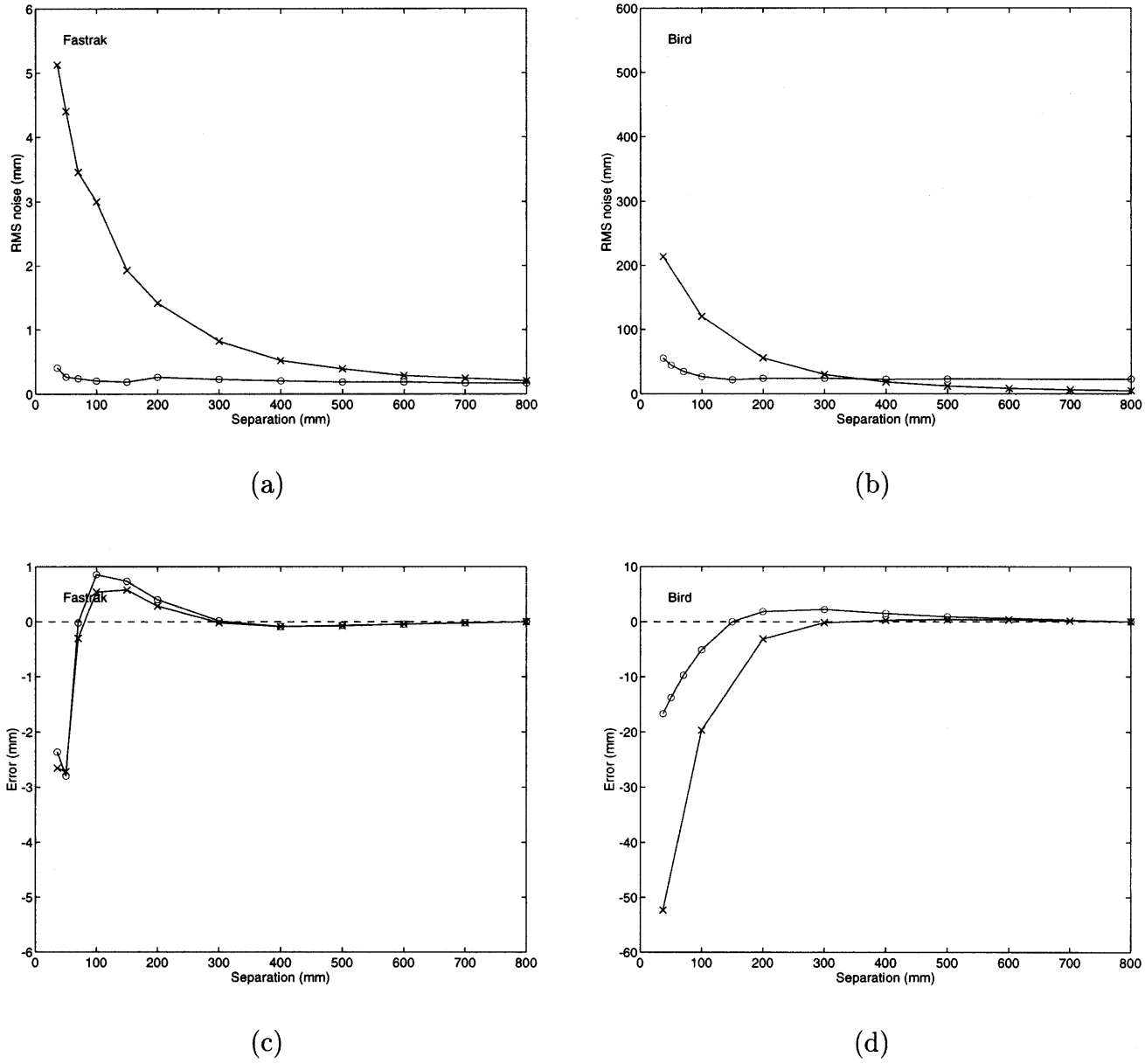

Figure 3. *The effect of receiver–monitor separation with sampling synchronized to the mains "x" or to the monitor "o" on position RMS noise for (a) Fastrak and (b) Bird, and position error for (c) Fastrak and (d) Bird. Note that the vertical scales of (a) and (b) differ by a factor of 100, and (c) and (d) differ by a factor of 10.*

In the case of the Fastrak, sampling synchronously at the monitor frequency reduced monitor interference to ambient noise levels at all tested monitor–receiver separations. When mains-synchronous sampling was employed (or asynchronous sampling for that matter), a separation of at least 800 mm was necessary to reduce monitor interference to ambient noise levels. At monitor–receiver separations of less than 200 mm, the position error exceeded 0.5 mm whether or not monitor-synchronous sampling was employed. Note that the carrier frequency of the Fastrak used was 12 kHz; CRT interference may be further reduced by using an 8 or 10

kHz model (Polhemus, Incorporated, Burlington, Vermont; private communication, 1997).

With the Bird, monitor-synchronous sampling effectively eliminated monitor interference, but at the cost of leaving the tracker open to ambient mains noise of some 25 mm RMS. In our particular experimental environment, with transmitter–receiver separation of 600 mm, mains-synchronous sampling was preferable for noise reduction at monitor–receiver separations of greater than 350 mm. Monitor-synchronous sampling was preferable at closer separations; however the error at this proximity began to exceed 2 mm. As with the Fastrak, a separation of at least 800 mm was necessary to reduce monitor interference to ambient noise levels with mains-synchronous sampling.

In conclusion, monitor-synchronous sampling can effectively eliminate monitor interference with the Fastrak, but offers little advantage with the Bird in the presence of other fields such as mains. With the latter, mains-synchronous sampling should in general be employed. As discussed earlier, it may not be necessary to actually synchronize to the mains if it is sufficiently stable, but simply to sample at a fixed rate of twice the nominal mains frequency and two-tap filter, for example. Alternatively, a higher-order low-pass filter that reduces both mains and monitor interference may be preferred, depending on the particular application.

4.3 Interference from Tracker Leads

It was noticed that on occasions when the tracker leads came within close proximity of the receiver or transmitter, a slight error was produced. To investigate this effect, the position and pointing error was measured, first when the transmitter lead was wound one turn around the receiver, and second when the receiver lead was wound one turn around the transmitter. In both cases, the lead was then drawn away until the error approached the ambient noise level, and the separation distance noted. Other combinations of leads and tracker components were explored.

Both trackers were found to be particularly sensitive (errors up to 500 mm) to the proximity of the transmitter lead to the receiver, and they required at least 400 mm separation to reduce the distortion to the level of ambient noise. Proximity of the receiver lead to the transmitter is another potential source of error for the Fastrak (errors up to 30 mm), but not the Bird. These effects are well in excess of distortion caused by the metal in the leads and are therefore due to unwanted electromagnetic coupling.

Through experimentation, no other combination of leads and tracker components could be found that produced errors above the ambient noise level.

4.4 Effect of Transmitter–Receiver Separation on Noise

According to the model developed in Section 2, the magnitude of noise due to interfering fields is expected to increase with the fourth power of the transmitter–receiver separation. To verify this relationship, noise measurements were made at varying transmitter–receiver separations d_{tr} with the sampling frequency synchronized to twice the mains frequency, and a two-tap filter applied. The results are plotted in Figure 4, with a superimposed line plot of a kd_{tr}^4 model that best approximates the position noise. Although the magnitude of the Bird's noise may be reduced by higher-order filtering (Ascension Technology Corporation, Burlington, Vermont; private communication, 1997), the relationship to transmitter–receiver separation will remain the same.

Note the saw-tooth appearance of the Bird noise at low transmitter–receiver separations. This appearance is due to stepwise increases in transmitter power with increasing d_{tr} up to about 300 mm. That is, a small increase in range can precipitate a step increase in transmitter power, with a resulting decrease in relative noise level.

5 Effect of Nearby Metals

As mentioned in Section 2, there are two metal-related phenomena that impinge on the performance of electromagnetic based trackers: eddy currents and ferromagnetism.

Eddy currents are induced in metals by a changing

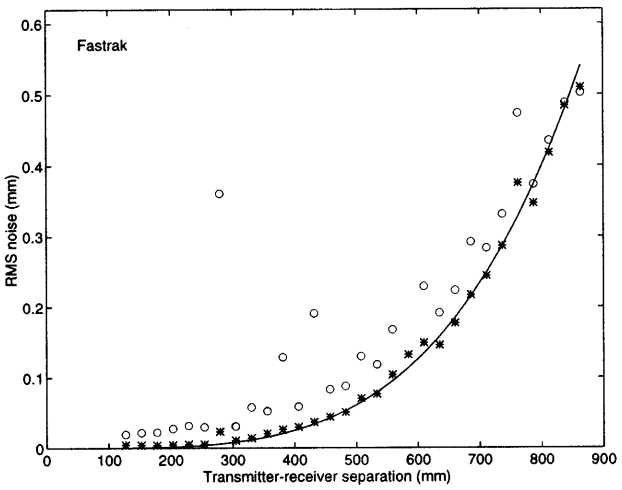

(a)

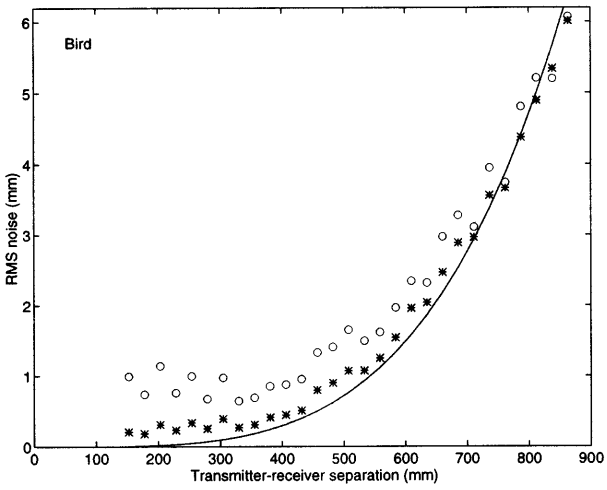

(b)

Figure 4. *The effect of transmitter–receiver separation on position RMS noise "*" and pointing RMS noise "o" for (a) Fastrak and (b) Bird, at different transmitter–receiver separations. Superimposed line of best fit is d_{tr}^4 model for position error. Note that the vertical scales of the two graphs differ by a factor of 10.*

magnetic field. AC-based trackers therefore induce eddy currents in nearby metals throughout each measurement period. DC-based trackers were developed in an attempt to alleviate this problem. Although eddy currents are still induced by the rising and falling edges of the DC pulse, delaying the field measurements until some time after the rising edge allows the eddy currents to decay significantly.

The magnetization field produced by ferromagnetic materials persists while the transmitter's field is applied, where the magnitude of the magnetization field depends on the permeability of the material. Ferromagnetic materials will therefore affect both AC and DC trackers. The permeability, furthermore, has a frequency dependency that generally diminishes with frequency; therefore, the Fastrak may be less affected by ferromagnetic materials than the Bird.

To investigate the effects that metals have on tracker accuracy, experiments were performed with small cubes of different metals. The relationship between the magnitude of the error and the separations between the metal, receiver, and transmitter is reported in Section 5.1. The dependence of error on size is considered for small metal objects in Section 5.2 and for larger metal objects in Section 5.3. Note that these experiments only considered the effect on error, as metals do not significantly affect the RMS noise.

5.1 Metal Cubes

The relationship between error and the separations of the transmitter, receiver, and metal was investigated in two experiments. In the first experiment, the relationship between error and the distance d_{tm} of the metal from the transmitter and the distance d_{mr} of the metal from the receiver, was investigated. The transmitter and receiver were separated by 600 mm and firmly attached to the table. The experimental setup is shown in Figure 5(a). Tracker sampling was synchronized to twice the mains frequency and a two-tap filter applied. The position and pointing errors, e_r and e_p, due to the presence of a 25-mm cube of metal (i.e., 25 mm $\times$ 25 mm $\times$ 25 mm) were measured as the metal was placed at various positions on the table. The experiment was repeated for a number of commonly available metals: mild steel, copper, stainless steel (316), brass, aluminum, and a ferrite (Philips 3C85). The effect of brass, stainless steel, and aluminum alloys will vary according to their composition. The results for mild steel are shown in Figure 6.

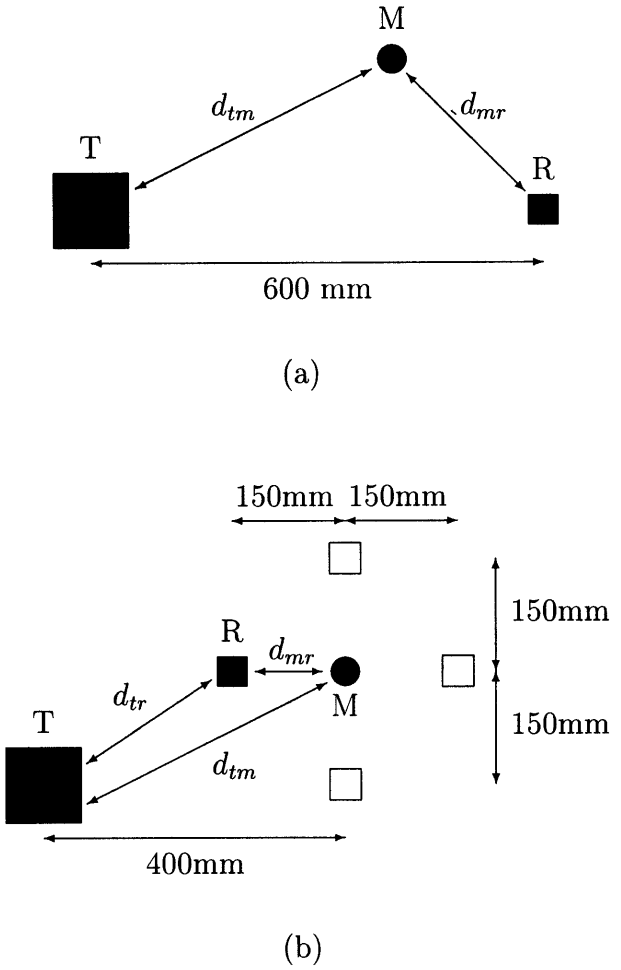

Figure 5. *Schematic diagram of the metal cubes experiment. In (a), the transmitter (T) and receiver (R) were securely fixed, and the metal (M) was placed at various positions, so as to vary* d_{tm} *and* d_{mr}*. In (b), the transmitter and metal were securely fixed, and the receiver was placed in four positions around the metal, so that* d_{tm} *and* d_{mr} *were kept constant while* d_{tr} *was varied. Note that the distances* d_{mr}, d_{tr}, *and* d_{tm} *are measured from the centers of their respective objects.*

Comparison of the measured errors with the superimposed line of best fit confirms an inverse cube relationship between the error and the separations d_{tm} and d_{mr}, as predicted from the analysis in Section 2. Curves of similar shape were obtained for the other metals tested and therefore not shown here.

In the second experiment the relationship between transmitter–receiver separation d_{tr} and metal induced error was determined. The transmitter and a cube of mild steel were fixed to the table, and the receiver was moved around the metal so that the distances d_{tm} and d_{mr} were constant. The experimental setup is shown in Figure 5(b). The result is shown in Figure 7, with a line of best fit that corresponds to d_{tr} to the fourth power. This result is consistent with the analysis in Section 2. Only the Fastrak was used for this investigation because the Bird's transmitter power is not constant with changing d_{tr}.

The results of these two experiments confirm that the position error varies as

$$e_r = \frac{k_r {d_{tr}}^4}{{d_{tm}}^3 {d_{mr}}^3} \tag{14}$$

and similarly for pointing error, where the proportionality constants k_r and k_p are functions of the properties of the metal.

From this model and the experimental data, Table 1 was generated to summarize the position and pointing error effects for 25-mm cubes of various types of metal placed 100 mm from the receiver in a line between the receiver and transmitter (d_{tr} = 600 mm).

From Table 1 and knowledge of the operating principles of the two trackers, some useful conclusions can be drawn about the effects of metals on the Fastrak and the Bird.

The Fastrak is sensitive to eddy currents and since all metals are conductors and produce eddy currents, the Fastrak was affected by all metals. The Bird was relatively insensitive to eddy currents induced in all metals with the exception of copper. Presumably the high conductivity of copper—resulting in larger eddy currents (Blood, 1990)—is such that the eddy currents are still significant when the Bird makes its measurements. Slowing the Bird's sampling rate would therefore further reduce the error due to the eddy current effect. With this exception aside, the Bird's algorithms are evidently successful at making it relatively insensitive to eddy currents; the effect of 25 mm cubes of stainless steel, brass and aluminum could not be measured during the experiment and were effectively invisible to the Bird.

Both trackers are sensitive to the ferromagnetic effects of metals. However, the trackers use different excitation

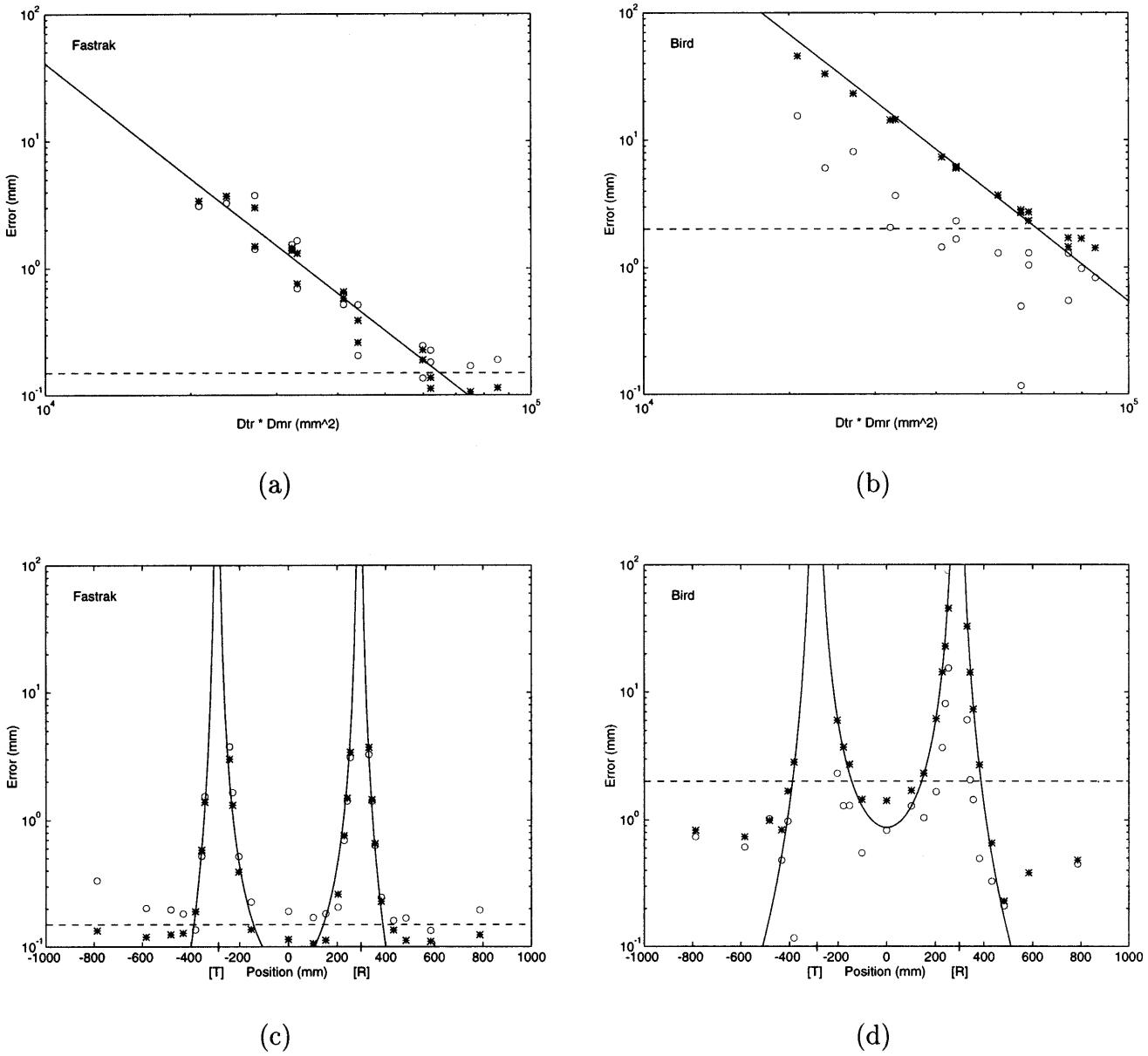

Figure 6. *The effect of a 25-mm mild steel cube on position error "*" and pointing error "o" at different transmitter–metal–receiver distances: error versus* $d_{tm}d_{mr}$ *for (a) Fastrak and (b) Bird; error versus position for (c) Fastrak and (d) Bird. Superimposed line of best fit is* $k/(d_{tm}^3 d_{mr}^3)$ *model for position error. Dashed line represents typical noise level in position (RMS mm) in absence of metal. Note that for clarity only the measurements made along the transmitter–receiver axis are shown, and that the position of the transmitter and receiver are labeled by [T] and [R] in (c) and (d).*

frequencies, and since the permeability of a metal depends on frequency, the effects of steel were different for the two trackers. With the Fastrak, the permeability of steel is low at 12 kHz and the ferromagnetic effects were consequently low, but steel is a good conductor, and the eddy current effects predominated. With the Bird, the eddy current effects of steel were low, but the permeability of steel at DC is high, and the ferromagnetic effects predominated. These observations are confirmed by the experiment with ferrite, a material with low conductivity, producing negligible eddy currents, but high permeability from DC to at least an order of magnitude greater

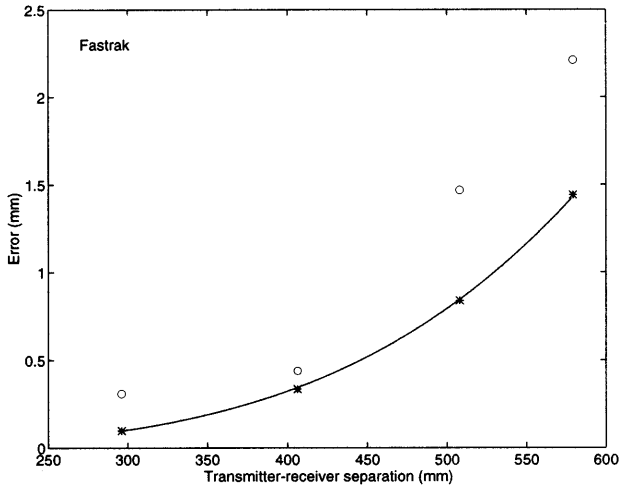

Figure 7. *The effect of a 25 mm mild-steel cube for the Fastrak on position error "*" and pointing error "o," with fixed transmitter–metal distance and fixed metal–receiver distance, at different transmitter–receiver distances. Superimposed line of best fit is best-fit* kd_{tr}^4 *model.*

Table 1. *Tracker Error (mm) due to 25-mm Cubes of Various Types of Metal Placed at 100 mm from Receiver, in a Position Between the Receiver and Transmitter.*[a]

	Fastrak		Bird	
Metal	Position	Pointing	Position	Pointing
Mild steel	0.3	0.3	5.4	1.7
Ferrite	1.8	2.5	3.6	2.1
Copper	1.2	1.1	1.3	1.5
Brass	1.2	1.2	—	—
Aluminum	1.2	1.1	—	—
316 stainless	0.8	0.6	—	—

[a]Transmitter–receiver separation was 600 mm, pointer length was 500 mm. Sampling was mains-synchronized and filtered.

than the operating frequencies of the trackers. Thus, ferrite produced significant ferromagnetic effects on both trackers.

With both trackers, the remedy to metal effects is distance: For small metal objects, an enormous gain can be achieved for a relatively small increase in distance from the metal. Ultimately, however, these devices suffer an increasing error sensitivity with transmitter–receiver separation.

5.2 Size Effects

The effect of metal size was investigated using square plates, 1-mm thick, of aluminum (nonferromagnetic) and mild steel (ferromagnetic) having 25-mm, 50-mm, 75-mm, and 100-mm sides. Each sheet was in turn placed at a distance of 90 mm from the receiver along the transmitter–receiver axis. The orientation of the sheet was chosen to produce the greatest errors, namely perpendicular to the transmitter–receiver axis. The transmitter–receiver separation was 600 mm, sampling was synchronized to twice the mains frequency, and two-tap filtering applied. For each sheet, the errors e_r and e_p were measured.

The results for the Fastrak are shown in Figure 8(a, c) and for the Bird in Figure 8(b, d). For the Fastrak, the position error increased approximately as L^3 for both metals, where L is the width of the sheet. The pointing error was less predictable. For the Bird, the position error increased approximately as L^2 for steel and was unmeasurable for aluminum. The pointing error was again less predictable, but smaller compared with position error.

The position error increases more rapidly with size for the Fastrak than the Bird. Since the Bird is relatively insensitive to eddy currents (e.g., the aluminum sheet was ''invisible''), the errors were probably due directly to the amount (L^2) of ferromagnetic material. The Fastrak, however, is also sensitive to eddy currents, and the increased (L^3) dependence was probably due to the relationship between eddy current effects (i.e., amplitude and time constant of decay) and metal size, as discussed by Blood (1990).

According to theory, it is the area (or projection) of the metal (i.e., what the transmitter ''sees'' and what the receiver ''sees''), rather than the volume, that determines the magnitude of the effect (Blood, 1990). To verify this theory, we repeated one of the size experiments (Fastrak with aluminum) with cubes having 25-mm, 50-mm, 75-mm, and 100-mm sides. Results are shown in Figure 9, which reveal an L^3 dependence, just as for sheets.

A consequence of steel-induced errors increasing faster with size for the Fastrak than the Bird is that it is not possible

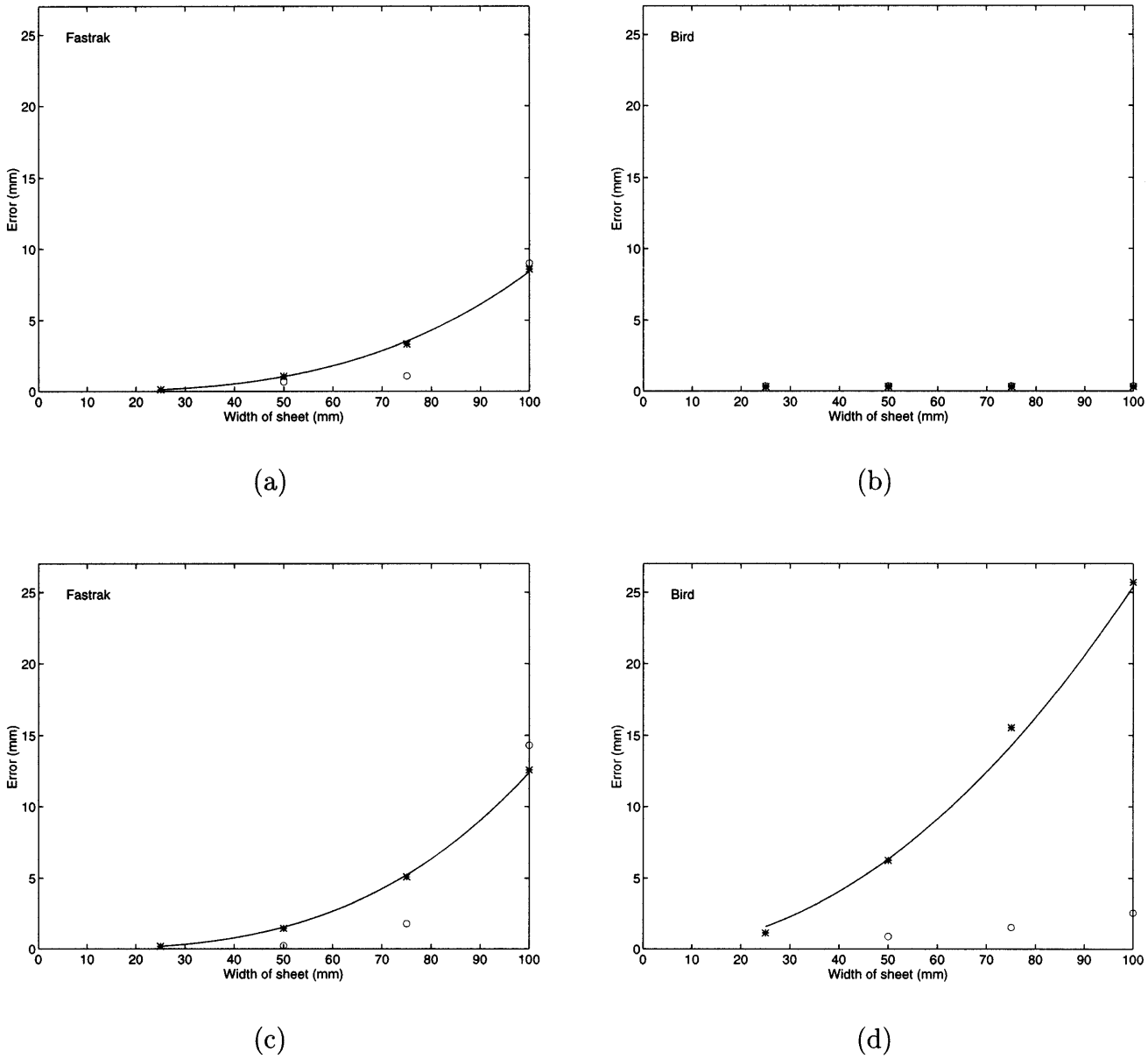

Figure 8. *The effect of different-sized sheets on position error "*" and pointing error "o" for aluminum sheets with (a) Fastrak and (b) Bird; and for steel sheets with (c) Fastrak and (d) Bird. The superimposed line of best fit in (a) and (c) is* L^3 *model for position error, and the superimposed line of best fit in (d) is* L^2 *model for position error.*

in general to say that one tracker is better than another in the presence of steel; it will depend on the size. For the small pieces of steel used in these experiments, the Bird had the greater errors. Extrapolating these results for our mild steel square plates, a plate with 200-mm sides would produce equal error in each locator; for plates larger than this, the Fastrak will have the greater errors.

5.3 Large Objects

The working environment of a magnetic tracker may include large metal objects such as desks and filing cabinets, as well as steel-reinforcing bars in floors or walls. To assess such effects, the errors e_r and e_p were measured in the presence of a long, rectangular steel

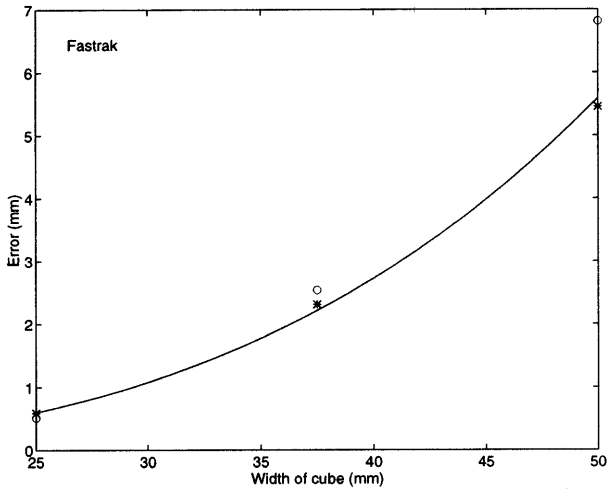

Figure 9. *The effect of different-sized aluminum cubes for the Fastrak on position error "*" and pointing error "o." The superimposed line of best fit is* L^3 *model for position error.*

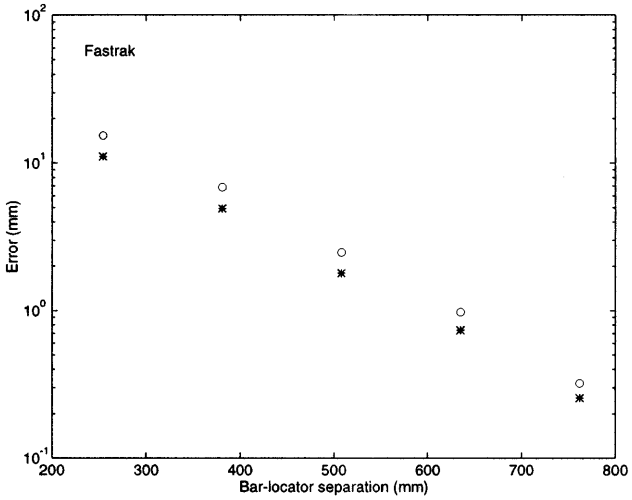

(a)

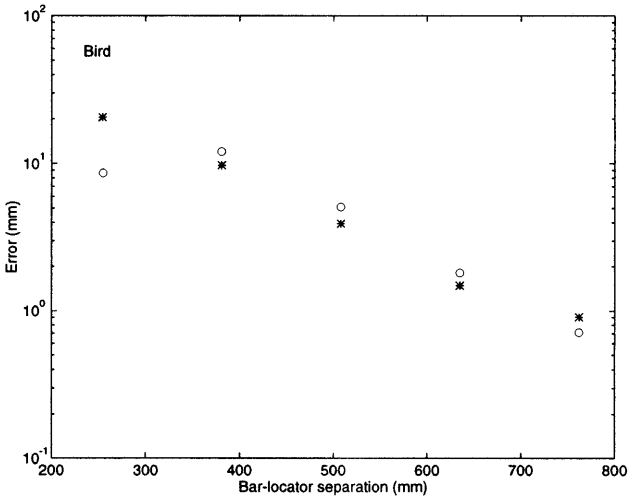

(b)

Figure 10. *The effect of a long, rectangular steel tube on position error "*" and pointing error "o," for (a) Fastrak and (b) Bird. The tube was positioned at various separations from the transmitter–receiver axis, lying parallel to the transmitter–receiver axis.*

tube and again with a steel filing cabinet. The rectangular steel tube was 1.75-m long with a 76-mm square cross section and 5-mm wall thickness. The filing cabinet was 1.3-m high, 0.50-m wide, and 0.57-m deep.

The steel tube and cabinet were positioned parallel to the transmitter–receiver axis, since this orientation produced the largest error measurements. They were then moved along a line perpendicular to the transmitter–receiver axis, and the errors were measured at several positions. The results are shown in Figure 10 for the tube and Figure 11 for the cabinet.

There is no obvious line of best fit for either case. This may be because at shorter separations the tube approximates an infinite line and the sheet approximates an infinite plane, whereas at greater separations the tube and cabinet resemble point sources.

These results also highlight the differences between the two trackers with different-sized objects, as discussed in the previous section. The size of the tube is such that the errors are greater for the Bird. Compare this finding to the results for the cabinet, where the Fastrak errors are much greater. Furthermore, if the metal objects contain closed conductive loops (e.g., grids of reinforcing bars in floors and walls, or loops in furniture), eddy current effects may be greater.

6 Conclusion

The experimental investigations described in this paper confirm that the inverse-cubed fall-off in signal with separation from the tracker's transmitter has major

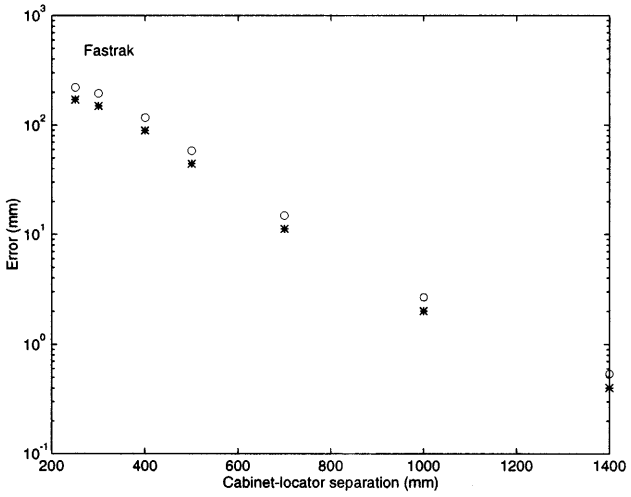

Figure 11. *The effect of a large steel filing cabinet on position error "*" and pointing error "o," for (a) Fastrak and (b) Bird. The filing cabinet was positioned at various separations from the transmitter–receiver axis, with the 1.3-m-by-1.57-m side facing the transmitter–receiver axis and lying parallel to it.*

ramifications for its performance. Errors due to external electrical fields and nearby metal increase as the fourth power of transmitter–receiver separation. Metal effects decrease as the third power of transmitter–metal separation and the third power of metal–receiver separation. If the metal can be moved away from both transmitter and receiver, the metal effect decreases as the sixth power of the distance. However, if the metal is in fixed proximity to the transmitter (e.g., part of a supporting table), then $d_{tm}{}^3$ is constant, $d_{mr} \approx d_{tr}$, and hence from (14) the metal's influence is effectively proportional to d_{tr}. Similarly, if the metal is in fixed proximity to the receiver (e.g., part of a stylus), then $d_{mr}{}^3$ is constant, $d_{tm} \approx d_{tr}$, and again from (14) the metal's influence is effectively proportional to d_{tr}.

The fundamental difference in operation of the two trackers leads to different relative sensitivity to interfering fields and metal. The Fastrak was found to be relatively insensitive to mains interference, and also to monitor interference with appropriate sampling synchronization. It was however found to be sensitive to both the eddy current and ferromagnetic effects of metals. The Bird was found to be relatively susceptible to mains or monitor interference, and required filtering and possibly mains-synchronous sampling to reduce this noise. It was found to be remarkably insensitive to nonferromagnetic metals and less sensitive than the Fastrak to large amounts of mild steel. However the relative sensitivity of the trackers to ferromagnetic materials depends on the size of the metal.

Interfering fields and metals in the operating environment are clearly significant factors that may affect the choice of magnetic tracker for a particular application.

Acknowledgments

The authors gratefully acknowledge the financial support of the New Zealand Foundation for Research, Science and Technology under PGSF grant DRF501. The authors would also like to thank both Ascension Technology Corp. and Polhemus Inc. for their comments on the manuscript.

References

Adelstein, B. D., Johnston, E. R., & Ellis, S. R. (1992). A testbed for characterizing dynamic response of virtual environ-

ment spatial sensors. *Proceedings, UIST Fifth Annual Symposium on User Interface Software and Technology,* 15–22.

Adelstein, B. D., Johnston, E. R., & Ellis, S. R. (1996). Dynamic response of electromagnetic spatial displacement trackers. *Presence: Teleoperators, and Virtual Environments, 5*(3), 302–318.

Barfield, W., & Furness, T. A. (1995). *Virtual environments and advanced interface design.* New York: Oxford University Press.

Blood, E. B. (1990). *Device for quantitatively measuring the relative position and orientation of two bodies in the presence of metals utilizing direct current magnetic fields.* U.S. Patent 4,945,305.

Bryson, S. (1992). Measurement and calibration of static distortion of position data from 3D trackers. *Proceedings SPIE—Stereoscopic Displays and Applications III,* 1669, 244–255.

Bryson, S., & Fisher, S. S. (1990). Defining, modelling, and measuring system lag in virtual environments. In *Proceedings SPIE—Stereoscopic Displays and Applications,* 1256, 98–109.

Burdea, G. C., Dunn, S. M., Immendorf, C. H., & Mallik, M. (1991). Real-time sensing of tooth position for dental digital subtraction radiography. *IEEE Transactions on Biomedical Engineering, 38*(4), 366–378.

Detmer, P. R., Bashein, G., Hodges, T., Beach, K. W., Filer, E. P., Burns, D. H., & Strandness, D. E., Jr. (1994). 3D ultrasonic image feature localization based on magnetic scanhead tracking: In vitro calibration and validation. *Ultrasound in Medicine and Biology, 20*(9), 923–926.

Ellis, S. R. (1991). Nature and origins of virtual environments: A bibliographical essay. *Computing Systems in Engineering, 2*(4), 321–347.

Emura, S., & Tachi, S. (1994). Compensation of time lag between actual and virtual spaces by multi-sensor integration. *Proceedings, 1994 IEEE International Conference on Multisensor Fusion and Integration for Intelligent Systems (MRI'94),* 463–469.

Ferrin, F. J. (1991). Survey of helmet tracking technologies. *Proceedings SPIE—Large-Screen-Projection, Avionic, and Helmet-Mounted Displays,* 1456, 86–94.

Kato, A., Yoshimine, T., Hayakawa, T., Tomita, Y., Ikeda, T., Mitomo, M., Harada, K., & Mogami, H. (1991). A frameless, armless navigational system for computer-assisted neurosurgery. *Journal of Neurosurgery, 74,* 845–849.

Liang, J., Shaw, C., & Green, M. (1991). On temporal-spatial realism in the virtual reality environment. *Proceedings, UIST Fifth Annual Symposium on User Interface Software and Technology,* 19–25.

Martin, R. W., Blood, E., Sheehan, F. H., Bashein, G., Otto, C. M., Derook, F., Filer, E., Li, X., & Detmer, P. R. (1993). A miniature position and orientation locator for three dimensional echocardiography. *Proceedings, Computers in Cardiology 1993,* 25–28.

Meyer, K., Applewhite, H. L., & Biocca, F. A. (1992). A survey of position trackers. *Presence: Teleoperators, and Virtual Environments, 1*(2), 173–200.

Raab, F. H., Blood, E. B., Steiner, T. O., & Jones, H. R. (1979). Magnetic position and orientation tracking system. *IEEE Transactions on Aerospace and Electronic Systems, AES-15*(5), 709–718.

Ramo, S., Whinnery, J. R., & Duzer, T. van. (1965). *Fields and Waves in Communication Electronics.* New York and London: John Wiley.

Stone, R. J. (1996). Position and orientation sensing in virtual environments. *Sensor Review, 16*(1), 40–46.

Williams, M. (1993). A comparison of two examples of magnetic tracker systems. In *Proceedings, Virtual Interfaces: Research and Applications* (pp. 14 / 1–19). Neuilly sur Seine, France: AGARD.

Wloka, M. M. (1995). Lag in multiprocessor virtual reality. *Presence: Teleoperators, and Virtual Environments, 4*(1), 50–63.